Sharing is encouraged

University of Exeter

Climatic warming changes to Northern European extreme temperature processes over the past 500+ years

John T Bruun
University of Exeter
j.bruun@Exeter.ac.uk

EGU23-15117
https://doi.org/10.5194/egusphere-egu23-15117
EGU General Assembly 2023

Supplementary

An update of ENSO

Stochastic and long term dynamic features appear present

Seasonal synchronisation is enhanced in the delay oscillator

Link to HEBE spectral features

Spectral signatures of ENSO

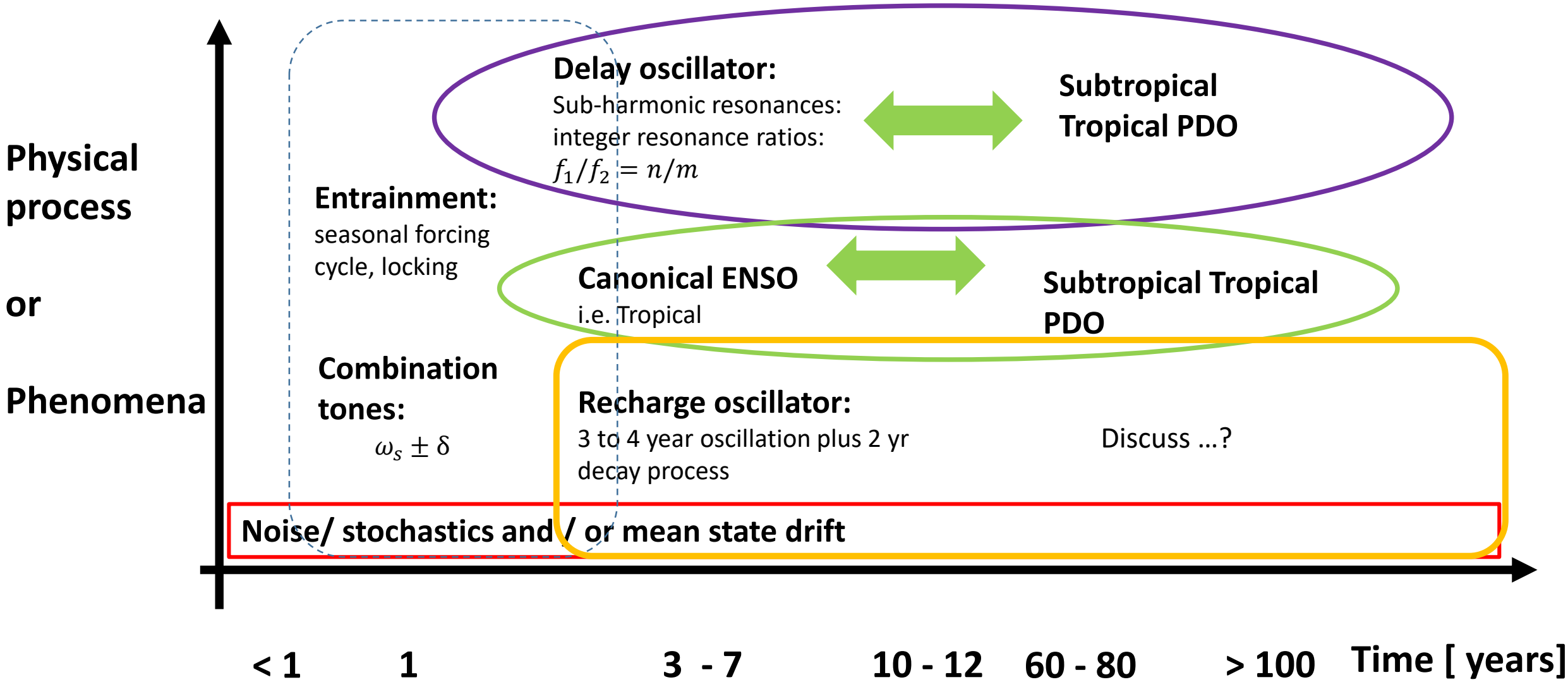

ENSO delay oscillator dynamic structure

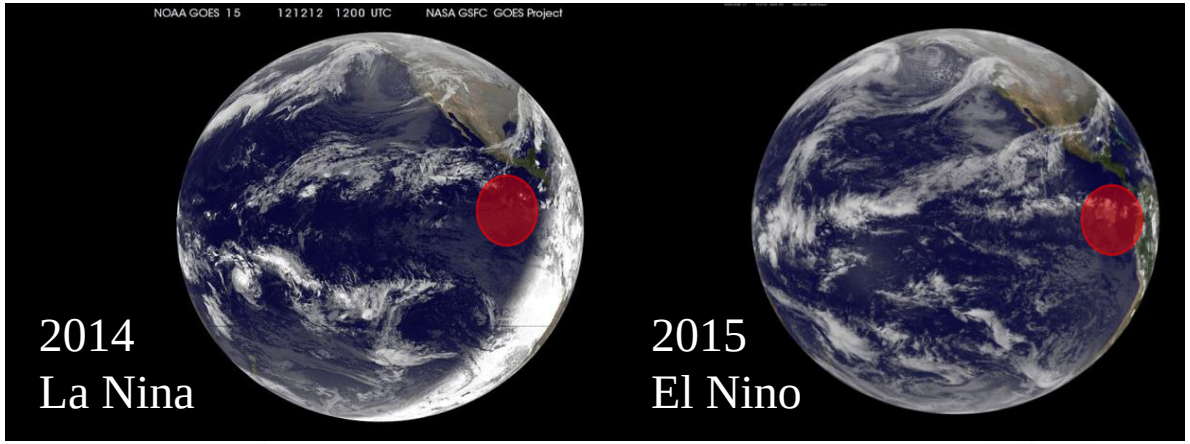

It is helpful for Tipping Element cascade to chaos studies and increasing turbulence physics properties.

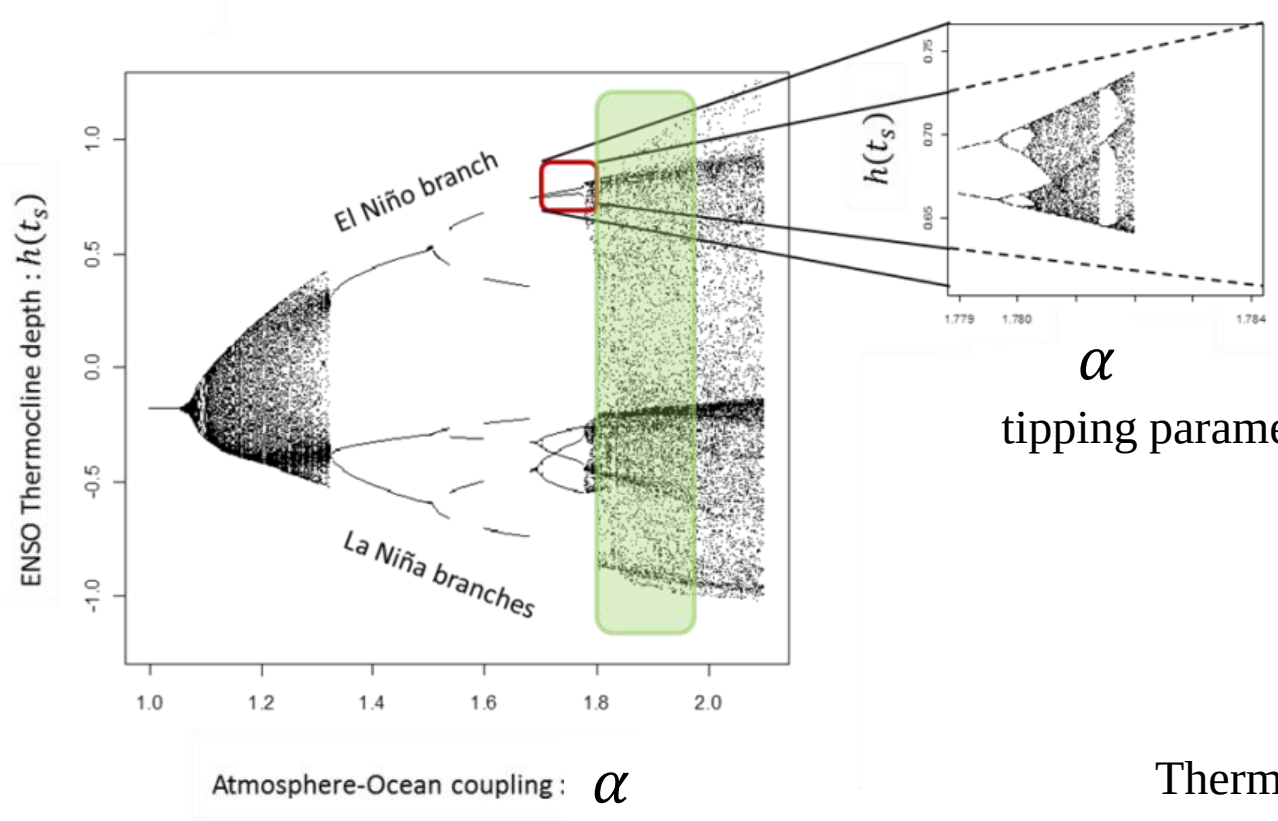

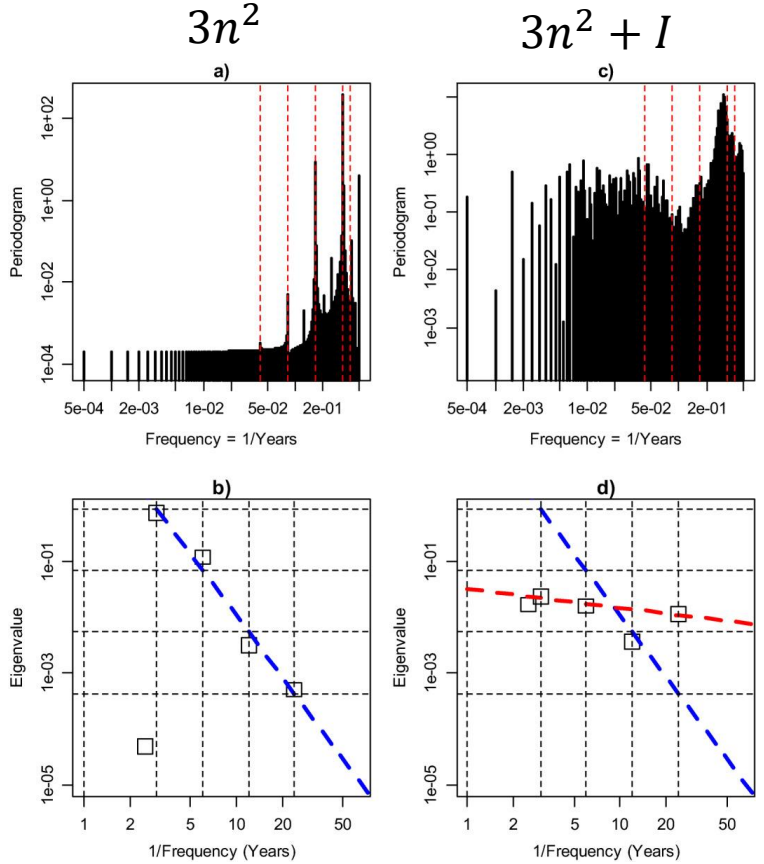

$$\frac{dh(t)}{dt} = aA\{h(t - \tau_1)\} - bA\{h(t - \tau_2)\} + c\cos(\omega_a t)$$

Thermocline depth $h(t)$ vibration

$$A\{h\} = \alpha\,(h - h^3)$$

Gives a 1d universal map of sub-harmonic resonance (Tziperman *et al* 1994; Bruun *et al* 2017**) and intermittency**
Equatorial wave guide physics

Period doubling to chaos gives an exact sub-harmonic resonance signature (which is Universal)

Feigenbaum constant α, *Period doubling subharmonic Eigenmode decay* $2n^2$ *: 8.7dB*, Feigenbaum, (1980)

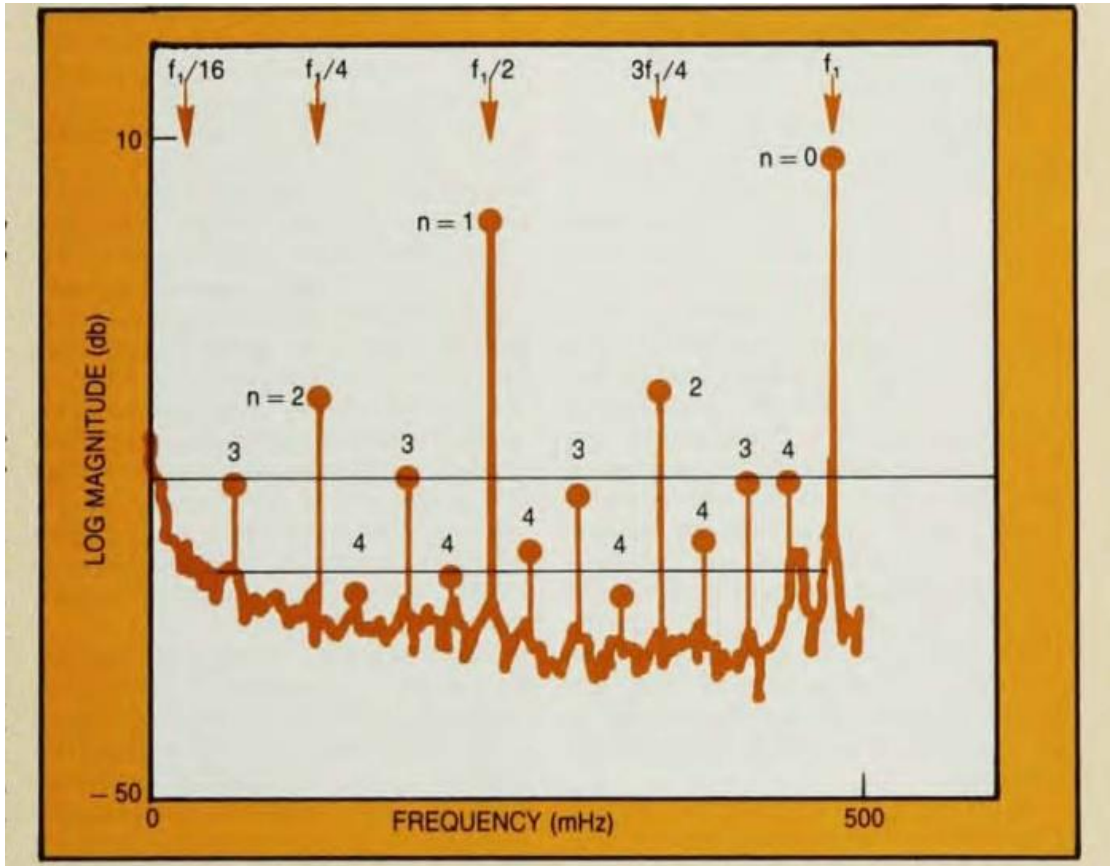

Experimental observation of period-doubling behavior leading to turbulence in Rayleigh–Benard flow. Libchaber and Maurer found frequencies f_1, $f_1/2$, $f_1/4$, $f_1/8$ and $f_1/16$. The set of subharmonic spectral peaks that have appeared at the nth period doubling are so labeled. Using the $n = 2$ peaks the theoretically predicted averages for the $n = 3$ and 4 peaks are drawn as horizontal lines. The two lines are 8.2 db apart. Figure adapted from references 3 and 4.

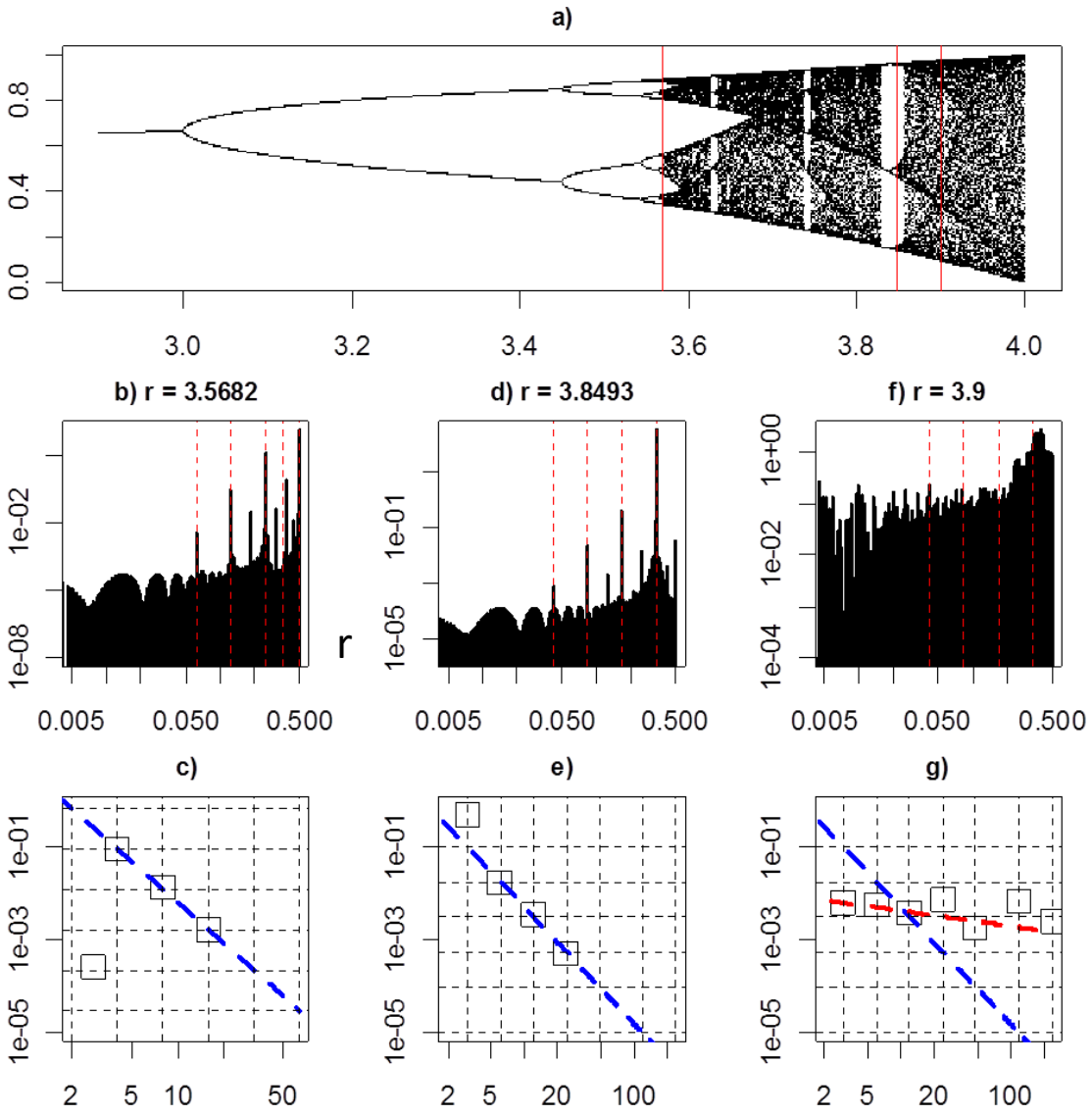

$3n^2, 3n^2 + Intermittency$, Bruun *et al* (2017)

Seasonal entrainment is enhanced in the intermittent tipping cascade and it includes combination tones (an emergent phenomena).

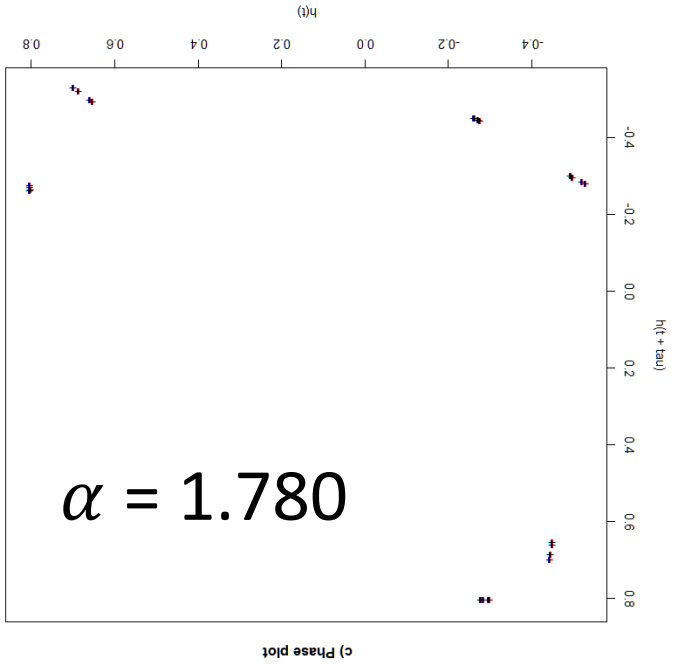

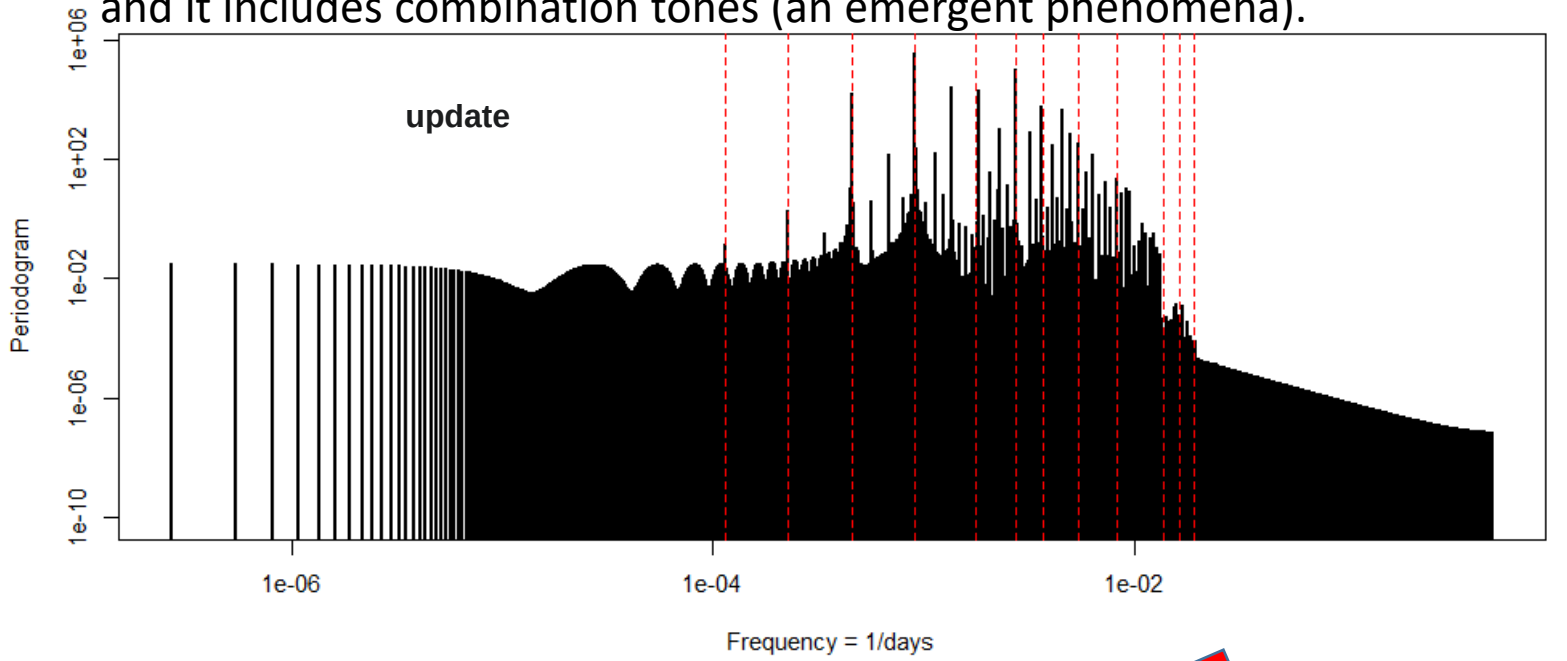

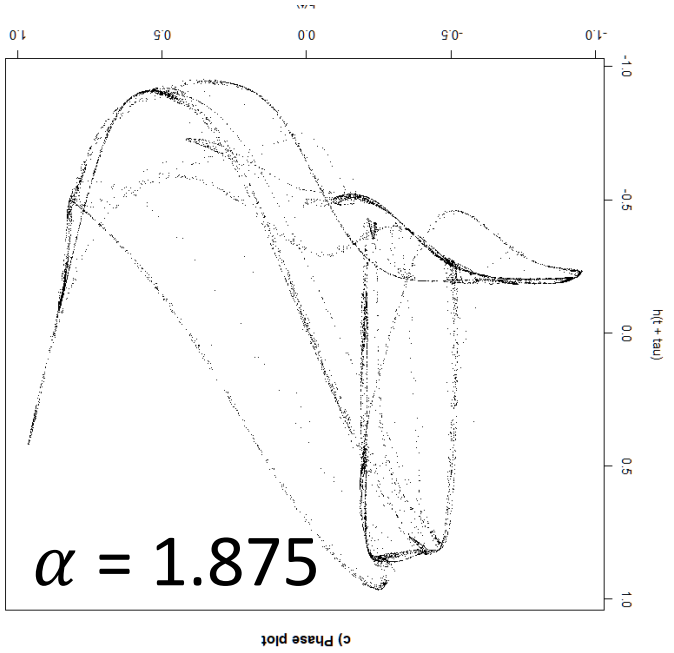

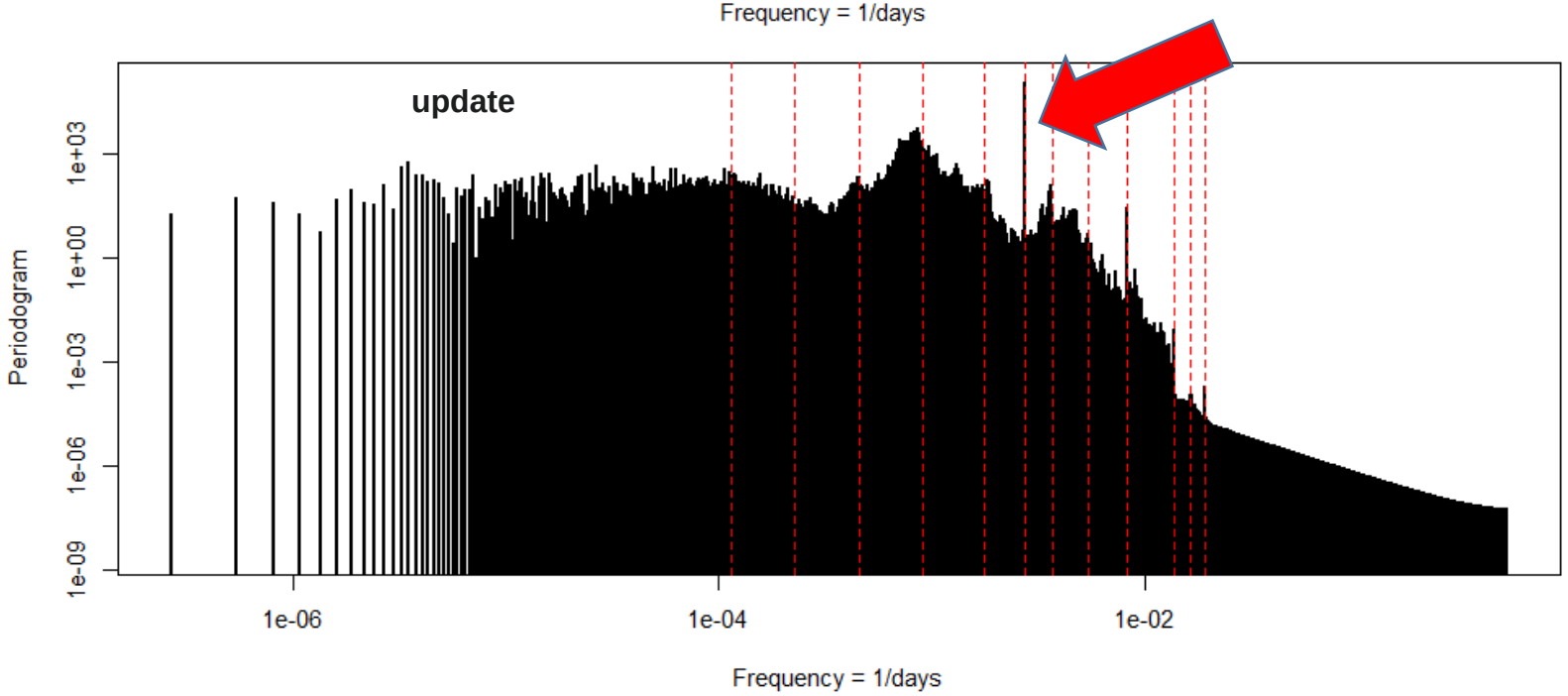

2000 yr burn, 10,000 year record

Lower frequency components : sub-tropical dynamics and tropical to sub-tropical coupling

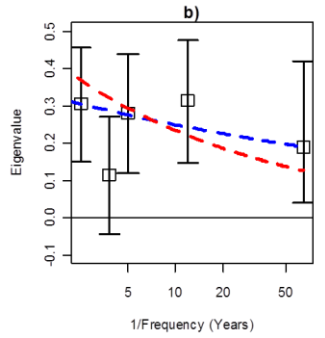

Fig. 7. Sketch of the mechanism of the PDO. SST anomalies can arise through reemergence of ENSO induced variability. Atmospheric noise excited Rossby waves which interact with the Kuroshio current, possible leading to path shifts leading also to SST anomalies, details in Newman et al. (2016).

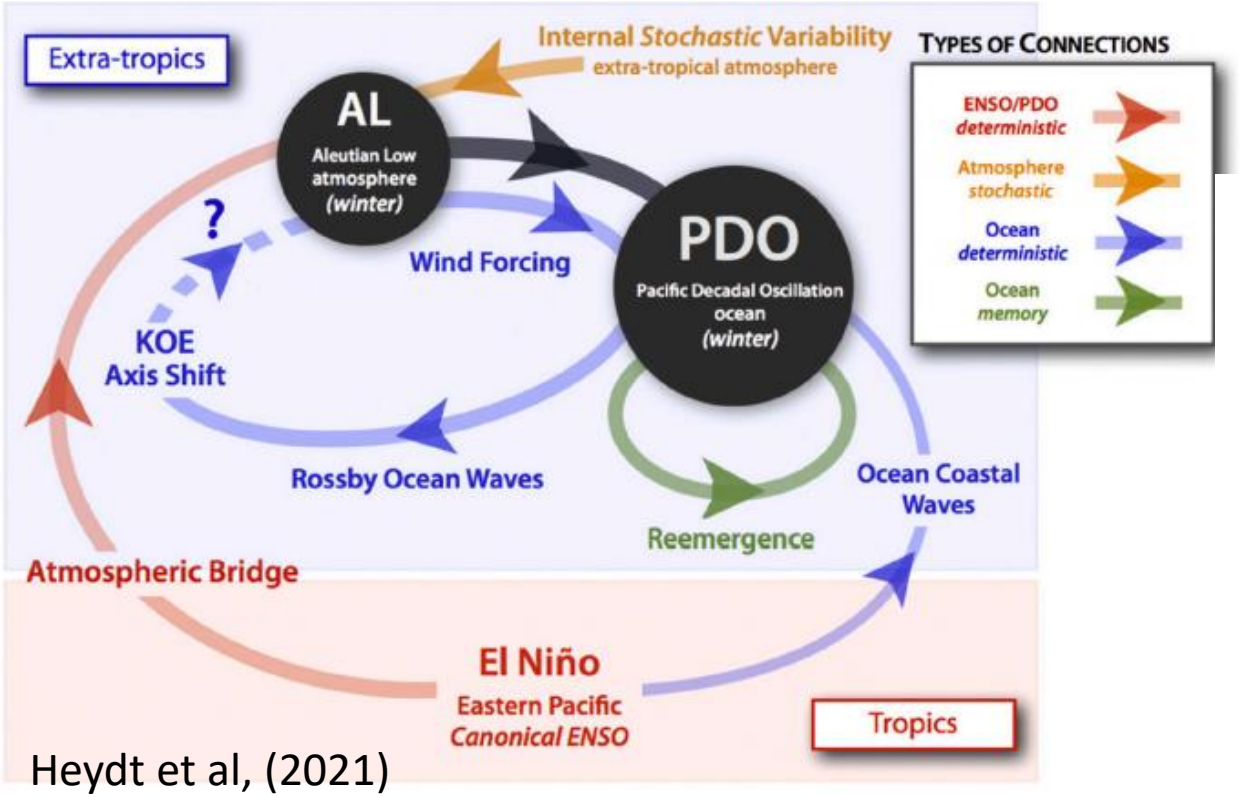

Heydt et al, (2021)

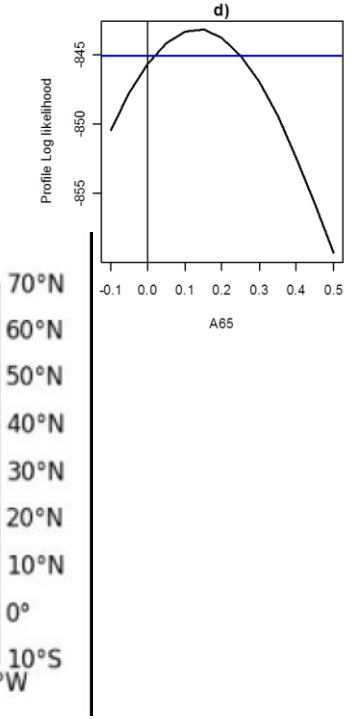

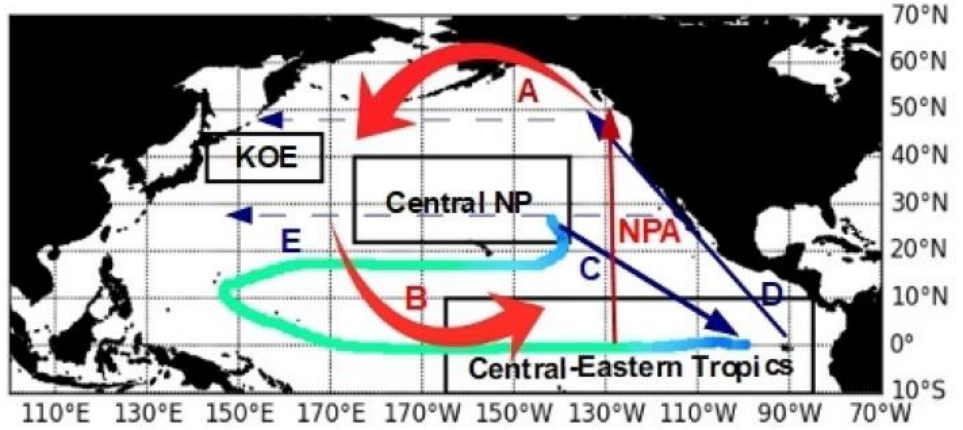

$$\frac{dT_{tr}}{dt} = ENSO(t) + \alpha^{O}\Delta T_{tr,ex}(t,\delta) + \beta^{A}T_{ex}\,(t)$$

The 65-75 year mode due to tropical-extratropical coupling. Period-three phase-locking between bi-decadal and penta-decadal modes, Skakála and Bruun (2018)

SOI update

Adding the most recent 5 years (2018 – 2023):

Canonical EL Nino 1 year mis-match (supports stochastic activation theory).

Persistent La Nina phase (supports modulated Heartbeat theory with a non-linear threshold 2015 to 2035).

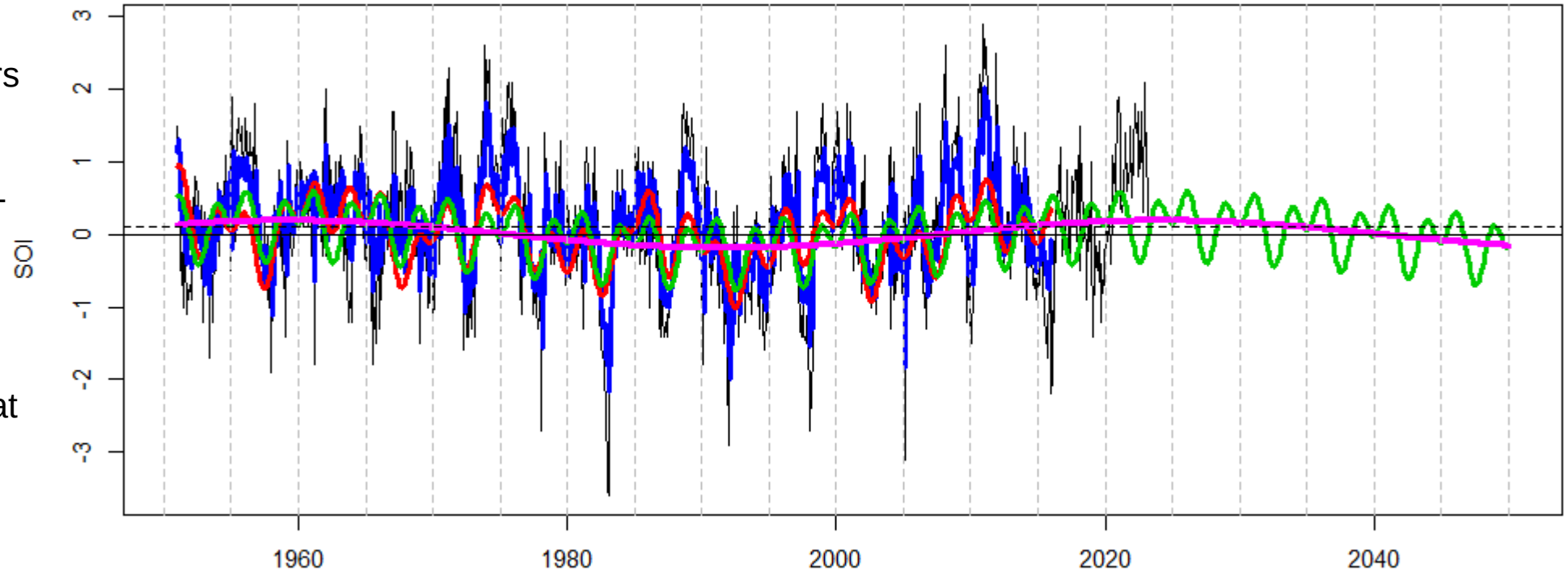

Any questions ….

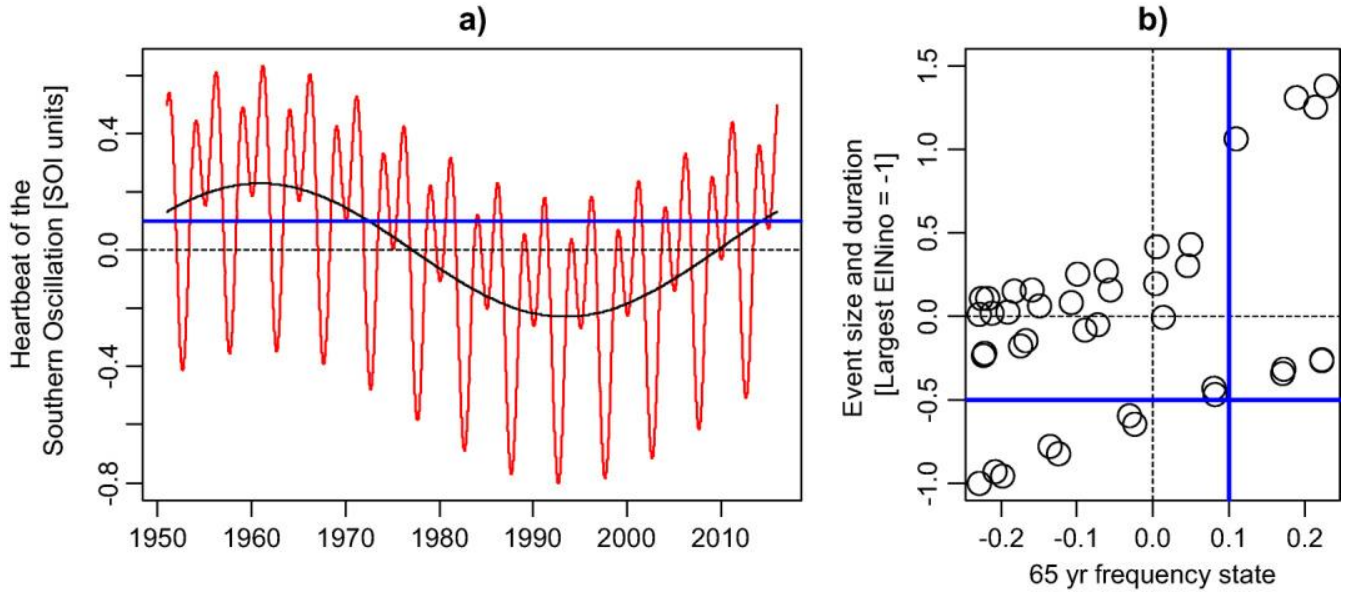

JGR Oceans, Volume: 122, Issue: 8, Pages: 6746-6772, First published: 26 July 2017, DOI: (10.1002/2017JC012892)

Heartbeat of the Southern Oscillation explains ENSO climatic resonances

ENSO dynamic structure plots from Bruun et al, 2017

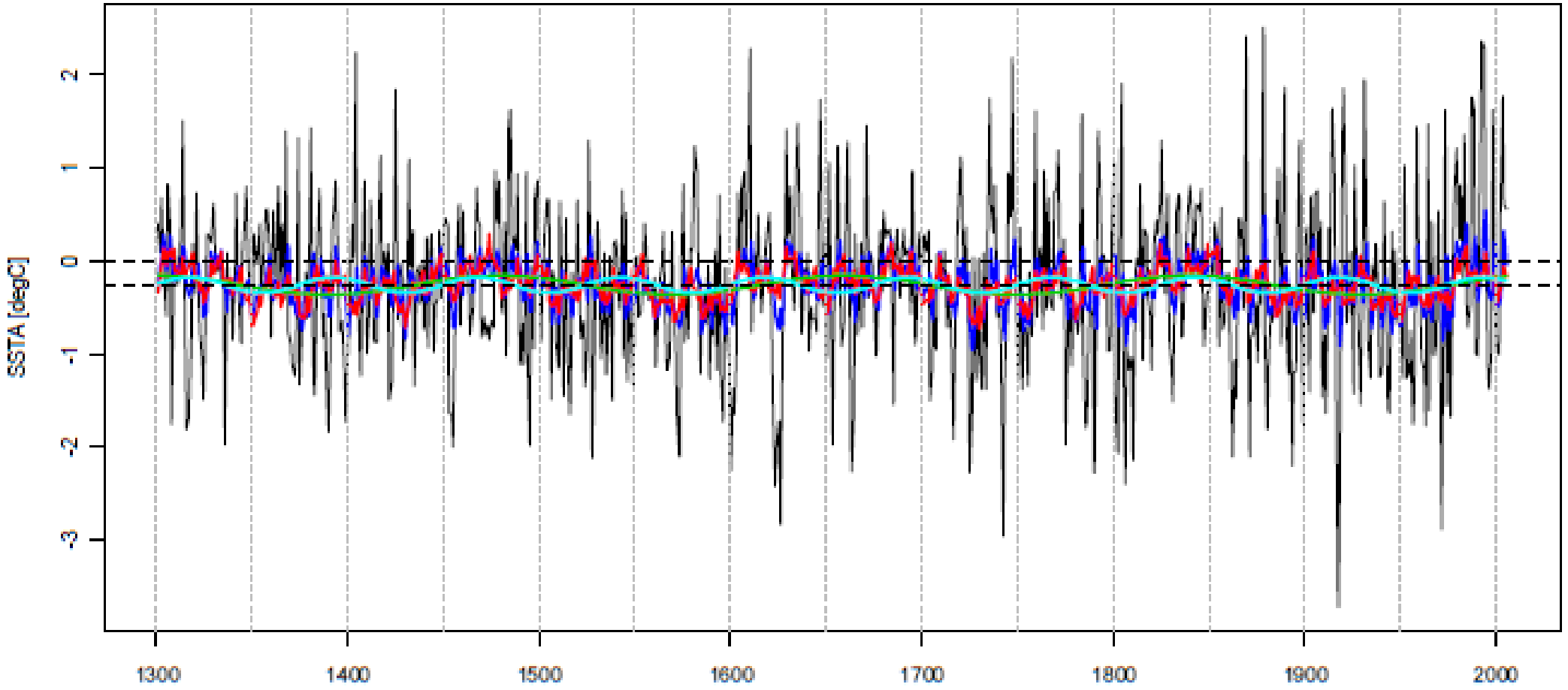

Figure S2. SSTA data and SSTA models: SSTA Signal analysis with DFSA. SSTA data (black line) estimated model: blue line including red-noise AR(1), red line -- the underlying combined frequency states, light blue line, the 75 year frequency state, green line the 180 year frequency state. Horizontal black dashed lines show SSTA mean of -0.26 and 0oC.

ENSO dynamic structure plots from Bruun et al, 2017

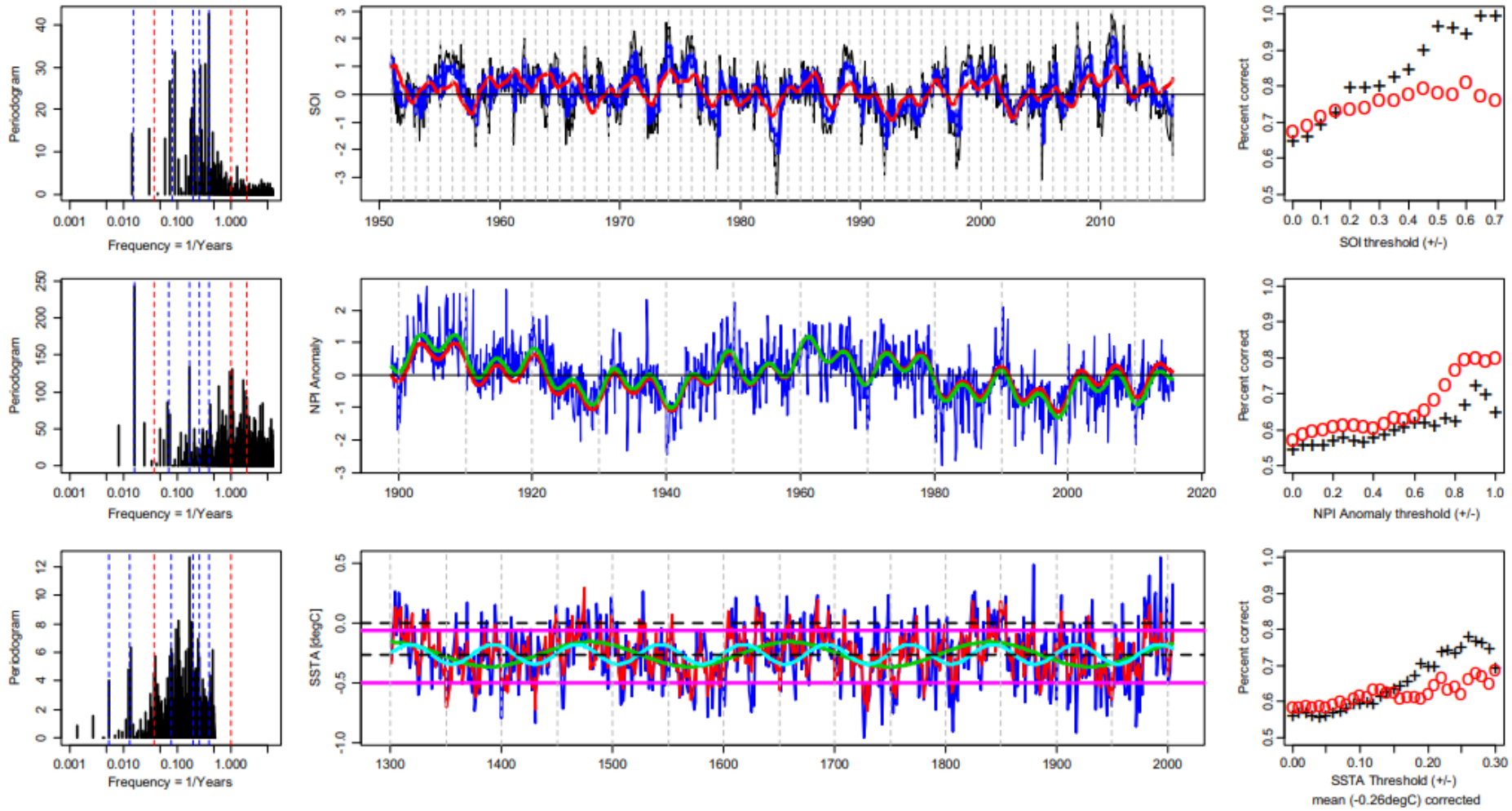

Figure 5. Frequency states of the ENSO process. Using BJTSA this shows the identification of dominant frequencies from data, the estimated frequency state models and the frequency state model skill assessment verses data. Southern Oscillation analysis: (a) spectrum, ω_{SOI} = {2.5, 3.8, 5, 12, 65} years; (b) SOI (black lines), estimated model (blue line including red-noise, AR(1), red line – the underlying combined frequency states), and (c) skill assessment true positive (red circles) and true negative (black +) verses increasing |SOI| threshold. North Pacific Index Anomaly analysis: (d) spectrum, ω_{NPIA} ={5.8, 14, 61} years; (e) estimated model: blue line including red-noise, AR(1), red line – the underlying combined frequency states, green line, the additional effect of including a trend, (f) skill assessment true positive (red circles) and true negative (black +) verses increasing |NPIA| threshold. Sea Surface Temperature Anomaly analysis: (g) spectrum, ω_{SSTA} ={2.5, 3.8, 5, 13, 27, 75, 180} years; (h) estimated model: blue line including red-noise, AR(1), red line – the underlying combined frequency states, light blue line, the 75 year frequency state, green line the 180 year frequency state. Solid thick purple lines show the thresholds indicated by skill analysis within which the frequency state models hold. (i) Skill assessment true positive (red circles) and true negative (black +) verses increasing |SSTA| threshold.

ENSO dynamic structure plots from Bruun et al, 2017

The supporting information shows the SSTA raw data and the variability structure of the residual. Following remarks by Li et al. [2013] the inter-decadal ENSO variance structure are examined. The variability of this indicates that either stochastic or underlying structural components of the system could cause the system to adapt its variance. We examine the absolute value of residual variance structure given by:

$$abs\ residual\ = |\ y_{SSTA} - f^{s}_{SSTA}| \qquad (18)$$

By applying DFSA to the residual series created from equation (16), we include 120 and 180 year cycles as shown in Figure S1. The raw SSTA data and the fitted model f^{s}_{SSTA} of Eq. (16) are shown in Figure S2 together with the raw SSTA data.

Figure S1.

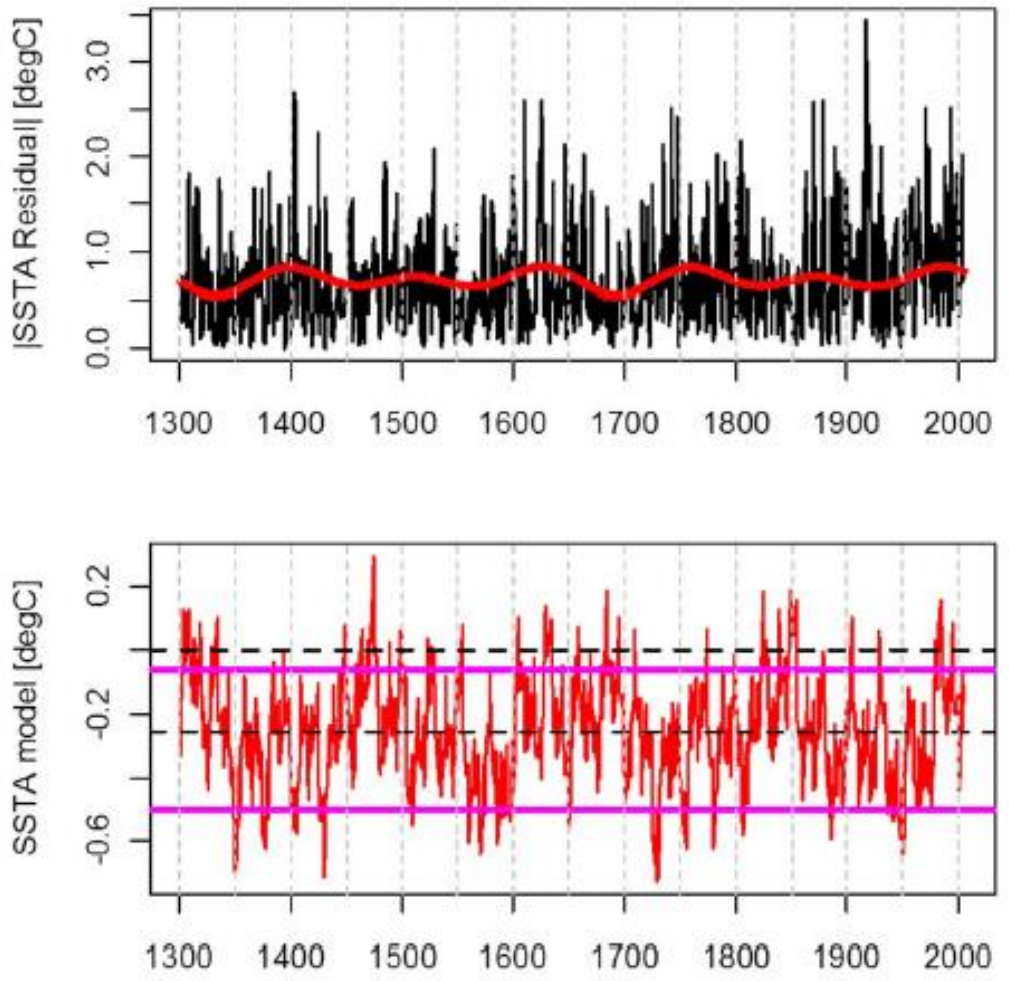

Figure S1. SSTA long term variance variability: SSTA |residual| analysis, a) black line: SSTA model |residual|, red line: |residual| model: long term cycles of 180 and 120 years modulate the variability. b) SSTA model (red line) with thresholds as shown in Figure 5.

References

Bruun, J. T., Icarus Allen, J., and Smyth, T. J. (2017), Heartbeat of the Southern Oscillation explains ENSO climatic resonances, *J. Geophys. Res. Oceans*, 122, 6746– 6772, doi:10.1002/2017JC012892.

Skákala, J., & Bruun, J. T. (2018). A mechanism for Pacific interdecadal resonances. *Journal of Geophysical Research: Oceans*, 123, 6549– 6561. https://doi.org/10.1029/2018JC013752

Peter C Young, P. C.; Allen, P. G. and Bruun, J. T. (2021), A re-evaluation of the Earth's surface temperature response to radiative forcing *Environ. Res. Lett*. 16 054068, DOI 10.1088/1748-9326/abfa50

Shi F, Duan A, Yin Q, Bruun JT, Xiao C, Guo Z. (2021) Modulation of the relationship between summer temperatures in the Qinghai-Tibetan Plateau and Arctic over the past millennium by external forcings, *Quaternary Research (United States)*, volume 103, pages 130-138, DOI:10.1017/qua.2021.3.

Bruun J.T., Evangelou S.N.. (2019) Anderson localization and extreme values in chaotic climate dynamics. *arXiv*, https://doi.org/10.48550/arXiv.1911.03998

Sudakov I, Vakulenko SA, Bruun J.T. (2022) Stochastic physics of species extinctions in a large population, *Physica A: Statistical Mechanics and its Applications*, volume 585, pages 126422-126422, 126422, DOI:10.1016/j.physa.2021.126422.

Tarran GA, Bruun J.T. (2015) Nanoplankton and picoplankton in the Western English Channel: abundance and seasonality from 2007–2013, *Progress in Oceanography*, volume 137, pages 446-455, DOI:10.1016/j.pocean.2015.04.024.

Bruun J.T, Tawn JA. (1998) Comparison of Approaches for Estimating the Probability of Coastal Flooding, *Journal of the Royal Statistical Society Series C: Applied Statistics*, volume 47, no. 3, pages 405-423, DOI:10.1111/1467-9876.00118.